

Metabolic Flux Balance Analysis of an Industrially Useful Microorganism *Corynebacterium glutamicum* by A Genome-Scale Reconstructed Model

Hiroshi Shimizu
Department of Bioinformatic
Engineering, Osaka University
2-1 Yamadaoka
Suita, Osaka 565-0871 Japan
+81-6-6879-7446
shimizu@ist.osaka-u.ac.jp

Yohei Shinfuku
Department of Bioinformatic
Engineering, Osaka University
2-1 Yamadaoka
Suita, Osaka 565-0871 Japan
+81-6-6879-7432
yohei_shinfuku@bio.eng.osaka-u.ac.jp

Masahiro Sono
Department of Bioinformatic
Engineering, Osaka University
2-1 Yamadaoka
Suita, Osaka 565-0871 Japan
+81-6-6879-7432
masahiro_Sono@bio.eng.osaka-u.ac.jp

Chikara Furusawa
Department of Bioinformatic
Engineering, Osaka University
2-1 Yamadaoka
Suita, Osaka 565-0871 Japan
+81-6-6879-7432
furusawa@ist.osaka-u.ac.jp

Takashi Hirasawa
Department of Bioinformatic
Engineering, Osaka University
2-1 Yamadaoka
Suita, Osaka 565-0871 Japan
+81-6-6879-7431
hirasawa@ist.osaka-u.ac.jp

ABSTRACT

Microorganisms have multi-hierarchical networks such as gene, protein and metabolites in the cells. *In silico* genome-scale metabolic models allow us to analyze characteristics of metabolic systems of organisms. In this study, we newly reconstructed a genome-scale metabolic model of an industrially useful microorganism, *Corynebacterium glutamicum*, based on genome sequence annotation and physiological data. The metabolic characteristics were analyzed using flux balance analysis (FBA). We simulated the metabolic fluxes both under aerobic and oxygen deprivation conditions. The predicted growth rates and production rates of organic acids as lactate and succinate exhibited good agreement with experimental data reported in the literatures. The genome-scale metabolic model provides a better understanding for evaluating metabolic capabilities and predicting metabolic characteristics of *C. glutamicum*. This can be a basis for *in silico* analyses of metabolic network.

Keywords

Genome Scale Model, Flux Balance Analysis, Metabolic Network

Permission to make digital or hard copies of all or part of this work for personal or classroom use is granted without fee provided that copies are not made or distributed for profit or commercial advantage and that copies bear this notice and the full citation on the first page. To copy otherwise, or republish, to post on servers or to redistribute to lists, requires prior specific permission and/or a fee.

Bionetics'08, November 25-28, 2008, Hyogo, Japan. Copyright 2008 ICST 978-963-9799-35-6.

1. INTRODUCTION

Recently, based on whole-genome information, the reconstruction of the genome-scale metabolic networks of a cell and application of it for metabolic flux balance analysis (FBA) [1, 2] has been conducted for many organisms, including each of the three major domains of the organisms, i.e., archaea [3], bacteria [4-7], and eukarya [8-10]. Flux balance analysis (FBA) is simple analysis of metabolic flux profiles by using a linear programming problem(LP) and the genome-scale models. Although the genome-scale metabolic models does not include kinetic information and cannot compute the detailed kinetic dynamics of metabolic reactions in a cell, these models enable us to describe the range of possible metabolic state based on constraints defined by the stoichiometry of metabolic reactions and transport steps at a steady state. Furthermore, we can obtain a solution, i.e. a set of all metabolic fluxes, which maximize an objective function using a linear programming. As an objective function, biomass production rate is generally adopted. It has been shown that the metabolic profiles calculated by maximization of biomass production can well describe those obtained experimentally in a number of organisms and environmental conditions, suggesting capability of organisms to maximize their growth rate by adaptation and evolution [11, 12]. Using the appropriate genome-scale metabolic network and the objective function to be maximized, FBA can be used to predict the relationship among genotype, environmental conditions and the product yields at the steady states, which can be utilized for improvement of microbial productions [13, 14].

A coryneform bacterium, *Corynebacterium glutamicum* is a facultative aerobic, Gram-positive bacterium capable of growing on a variety of sugars or organic acids [15]. This organism can produce various amino acids, such as glutamate [16] and lysine [17] with high efficiency, thus it is widely used for the large-scale production of amino acids by fermentation [18]. Furthermore, production of ethanol and organic acids such as lactate and succinate using *C. glutamicum* under oxygen deprivation condition has recently proposed [19]. Due to its importance for bioproduction, *C. glutamicum* has been chosen as one of the target microorganisms for metabolic engineering purposes [20]. Construction and exploration of appropriate *in silico* metabolic models were highly desired for discussion of cellular behavior to adapt different conditions.

In this paper, we presented the reconstruction of genome-scale metabolic model of *C. glutamicum*. Metabolic reactions and other parameters for biomass were collected using databases and literatures. After reconstruction of the model, we performed FBA simulations to verify the results of simulations using experimental data, under aerobic and oxygen deprivation conditions. This suggests *C. glutamicum* change the metabolic fluxes under different environmental conditions so that the biomass production rate is maximized under given environmental conditions.

2. GENOME-SCALE MODEL

2.1 Metabolic Pathways Reconstruction

All known reactions in *C. glutamicum* metabolic network were collected by a search of public databases and scientific publications. The basis of the genome-scale metabolic network was pathways in the Biocyc database collection [21] (www.biocyc.org) for *C. glutamicum*. The information on the genomic catalogue at the Kyoto Encyclopedia of Genes and Genomes database (KEGG; www.kegg.jp) for *C. glutamicum* was also referred. As for the reactions missing from these database but required for biomass production, we added them based on literatures [22].

2.2 Biomass Composition

To simulate the metabolic fluxes, the biomass composition was necessary information. It was estimated to account for the consumption of precursors and building blocks for cellular growth [22-26]. Biomass synthesis was represented by a linear combination of 43 components including amino acids, DNA, RNA, lipids, and cell envelope components. The energy requirement for cellular growth was also considered by taking into account ATP consumption in the biomass composition [27]. From the biomass composition, an elemental biomass composition was calculated as, $C_{37.8} H_{61.5} O_{18.5} N_{8.1} P_{0.30} S_{0.23}$.

2.2 Computational Method

Metabolic fluxes of *C. glutamicum* metabolic network were calculated by using flux balance analysis (FBA). All calculations including linear programming problem were performed using

commercially available software Lindo (Lindo Systems Inc.) and Matlab (Mathworks Inc.).

For a metabolic network consisting M metabolites and N metabolic reactions, assuming pseudosteady state of metabolites concentrations, the stoichiometric balance of metabolic fluxes was represented by the following equation:

$$S \cdot v = 0$$

where S represents $M \times N$ stoichiometric matrix and v indicates a flux vector with length N . We set the upper and lower bounds, α_i and β_i for i -th flux, to define constraint for maximal enzymatic rate, irreversibility of reaction, or constant uptake from the environment. To achieve a single solution of fluxes, we maximized or minimized a suitable objective function under above constraints. For FBA, we adopt the biomass production rate mentioned above as the objective function to be maximized.

For all the simulations in this manuscript, glucose was chosen as a sole carbon source, and the following external metabolites were allowed to freely transport through the cell membrane: CO_2 , H_2O , SO_3 , NH_3 , and PO_4 .

3. RESULTS AND DISCUSSION

3.1 Development of the Genome-Scale Model

We developed a genome-scale metabolic network for *C. glutamicum* ATCC 13032, whose genome DNA sequence was determined by two independent research groups [28, 29], including of 277 genes, 499 metabolic reactions and 438 metabolites. The entire reaction data was provided as a supplemental material of this report. A total of 406 reactions on the BioCyc database collection were included into the model, while the remaining 65 reactions were added to fill the gap in metabolic pathways for biomass production, based on physiological considerations. The basic characteristics of the reconstructed metabolic network were presented in Table 1. From the entire set of reactions, 471 correspond to intracellular reactions while 34 were the fluxes for transport through the membrane. The model includes 438 intracellular metabolites and 18 extracellular metabolites. Transport processes were added to the model based on the BioCyc database collection, transport classification database (TCDB; www.dcdb.org), and the inference from physiological considerations and genome annotations [22].

The reconstructed metabolic network of *C. glutamicum* has several distinguishing characteristics from other microorganisms. The cell envelope of *Corynebacteria* and *Mycobacteria* has a unique structure consisting of a covalently linked mycolic acid, arabinogalactan, and peptidoglycan complex (MAPc) [30].

Table 1. Basic Features of the Developed Model

Feature	Property
Genome characteristics	
Genome length(bp)	3282708 bp
G+C content (%)	53.80%
No. of ORFs	3432
Coding sequences(CDS) total	3002(100%)
CDS encoding annotated proteins	2489(83%)
In silico metabolic networks	
No. of genes included	277
No. of associated reactions	406
No. of other reactions	93
No. of metabolites	438
No. of internal fluxes	499
No. of exchange fluxes	34
Dimensions of S (metabolites by reactions)	438 by 533

To represent the characteristics of cell envelop biosynthesis, we introduced metabolic reactions for MAPc biosynthesis into the model. The MAPc was considered as the biomass component, whose coefficient was calculated based on the experimental results of previous studies [31, 32]. Also in the central metabolic pathway, the reconstructed model of *C. glutamicum* lacks some metabolic reactions which are commonly utilized in metabolic networks of other bacteria, such as NAD dependent malate dehydrogenase and pyruvate-formate lyase. In amino acids biosynthesis pathways, *C. glutamicum* lacks threonine aldolase and glycine C-acetyltransferase, both of which are involved in the conversion of threonine into glycine. These distinguishing characteristics of the metabolic pathways are responsible to represent the flux profile of *C. glutamicum*.

3.2 Analysis of Metabolic Flux Profiles under Aerobic and Oxygen Deprivation Conditions

We compared growth and metabolic profiles obtained by simulation results of FBA with those of experimental data under aerobic and oxygen deprivation conditions. In the case of aerobic condition, we compared the FBA calculation of fluxes and the growth rate with the experimental results shown in previous report [33]. The glucose uptake rate in the simulation was set to 15.03 mmol/g cell dry weight (DW)/h, which was the experimentally observed value, while the uptakes of other metabolites, including oxygen, allowed to freely be transported through the cell envelope. As results, we found that the FBA result showed good agreement with experimental data. For example, when glucose uptake rate was set to 15.03 mmol/DW/h, the FBA calculation resulted that the specific growth rate is 0.4 1/h, while the experimentally obtained specific growth rate is 0.38 1/h. Also, the simulation showed that oxygen uptake rate is 30.3 mmol/DW/h in this maximal growth condition, and the experimental result of oxygen uptake rate is 29.01.

In the case of oxygen deprivation condition, we set glucose uptake rate in FBA as 3.03 mmol/gDW/h, to compare with the experimental results in the previous report [18] for the reference, while oxygen uptake rate was set to zero to represent the oxygen deprivation condition. Also, we found that the FBA results showed good agreements with the experimentally observed metabolic fluxes. For example, lactate and succinate production rates under optimal growth assumption were calculated as 3.70 and 0.99 mmol/gDW/h, respectively, while the experimentally observed production rates were 5.68 and 0.55 mmol/gDW/h. Here, an important point was that the production rate of organic acids to the glucose uptake can be predicted with high precision only by optimizing biomass production rate.

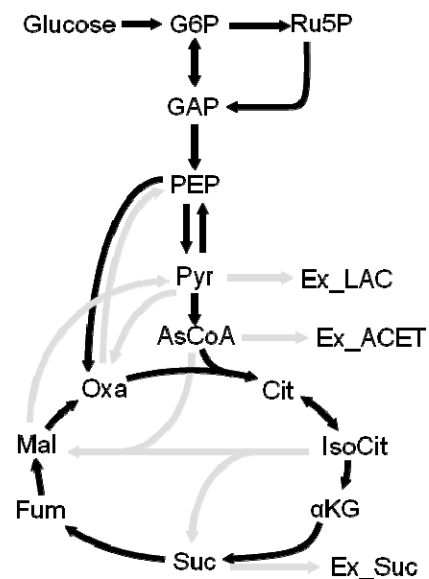


Fig. 1 Metabolic flux profiles calculated by FBA. Flux profiles of *C. glutamicum* under aerobic condition. Solid arrows indicate active metabolic fluxes. Gray arrows indicate inactive metabolic fluxes.

The FBA results of flux profiles under both aerobic and oxygen deprivation conditions are schematically shown in Fig. 1 and Fig.2. In the figures, active metabolic pathways were represented by solid arrows. As expected, under aerobic condition, glucose is metabolized into pyruvate via the glycolytic pathway, which is mainly converted to acetyl-CoA and enters the tricarboxylic acid (TCA) cycle. In contrast, under oxygen deprivation condition, large portion of pyruvate converted from glucose via glycolysis is utilized for lactate production, while some fraction is converted into oxaloacetate (OAA) by anaplerotic pathway. OAA is subsequently metabolized to succinate by the reductive TCA cycle. The use of the reductive TCA cycle to produce succinate is consistent with experimental results reported [18].

Next, we investigated the FBA simulation results of the production rates of organic acids and carbon dioxide as the function of oxygen uptake rate. In this simulation, the production rates were calculated under the fixed glucose uptake rate (15

mmol/gDW/h). As a result, the changes in production rates can be classified into three phases, named phase I, II, and III. In the phase I, cells produce lactate and succinate under relatively low oxygen uptake rate condition. In this phase, the production of these organic acids is necessary to oxidize NADH which is produced in the glycolytic pathway. In the phase II, with the increase in oxygen uptake rate, lactate production rate decreases, while acetate production rate increases. Here, the increase in NADH oxidation activity in the electron transport chain results in acetate production rather than lactate production. Here, the acetate production is preferred since the ATP production coincidentally occurs with acetate production and the ATP production is one limiting factor for biomass production. In this phase, metabolic fluxes of both oxidative and reductive TCA cycle are relatively small. In the aerobic condition (phase III), the oxidative TCA cycle becomes active, while a large portion of carbon derived from glucose is converted into carbon dioxide.

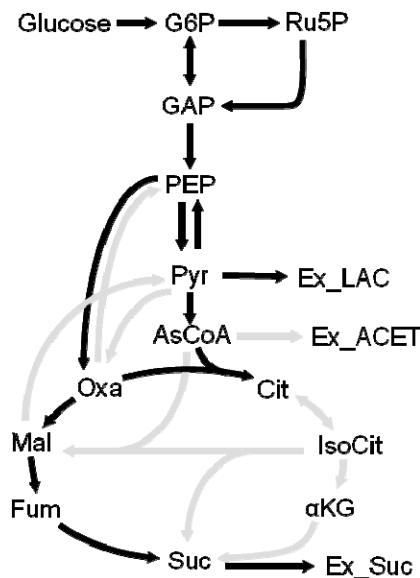


Fig. 2 Metabolic flux profiles calculated by FBA. Flux profiles of *C. glutamicum* under oxygen deprivation condition. Solid arrows indicate active metabolic fluxes. Gray arrows indicate inactive metabolic fluxes.

3.3 Comparison of Metabolic Flux Profiles between *C. glutamicum* and *Escherichia coli*

To investigate how FBA results and experimentally observed metabolic fluxes depend on the characteristics of metabolic network, we compared FBA results of two species with different metabolic networks, i.e., *C. glutamicum* and *E. coli*. As for genome-scale metabolic model of *E. coli*, we used iJR904 reported [34]. The FBA result of *E. coli* in aerobic condition, i.e. unconstrained oxygen uptake, was similar to that of *C. glutamicum*. In Fig.3, the FBA result of *E. coli* in oxygen deprivation condition is shown. The parameters in this FBA were set to be identical to those in the FBA of *C. glutamicum* in oxygen

deprivation condition, i.e., glucose and oxygen uptake rates are set to 3.03 and 0 mmol/gDW/h, respectively.

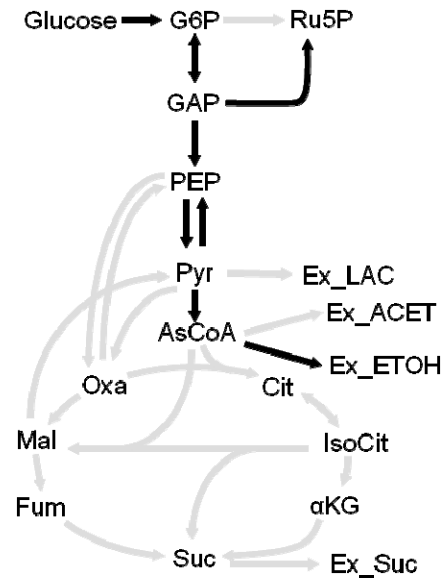


Fig. 3 Metabolic flux profiles calculated by FBA. Flux profiles of *E. coli* under oxygen deprivation condition. Solid arrows indicate active metabolic fluxes. Gray arrows indicate inactive metabolic fluxes.

As shown, there were two major differences between flux profiles of *C. glutamicum* and *E. coli*. One was difference in products secreted into the outside of the cells. As discussed above, according to the FBA calculation in the oxygen deprivation condition, *C. glutamicum* cells secrete lactate and succinate into the outside of the cells, which was consistent with experimental results. In contrast, the result of FBA of *E. coli* exhibits that the cells secrete formate and ethanol under the same condition.

Another difference in the metabolic profiles between *C. glutamicum* and *E. coli* was the fluxes of pentose phosphate pathway (PPP). In the case of *C. glutamicum*, the FBA result indicates that oxidative PPP is active under the oxygen deprivation condition. In contrast, non-oxidative PPP is utilized in the case of *E. coli*.

It is worth noting that using flux analysis based on the ¹³C labelling, the activation of non-oxidative PPP in *E. coli* metabolic pathways was experimentally demonstrated [35], as expected from FBA calculation.

In this study, we developed a genome-scale metabolic model of *C. glutamicum*, which is industrially important for production of amino acids and useful chemicals. Using the genome-scale model, we performed the FBA to understand the characteristics of metabolic network. As results, we found that the results of FBA showed good agreements with experimental results as shown in Tables 3 and 4, especially production rates of organic acids under oxygen deprivation condition. We also investigated the difference in FBA results between *C. glutamicum* and *E. coli*. As shown in

Figs.2 and 4, the differences in metabolic flux profiles between *C. glutamicum* and *E. coli* reflect the difference in metabolic networks of them. It should also be noted that, these differences in FBA results are consistent with experimental data. We expect that such comparative analysis of genome-scale models and experimental data enable us to capture the characteristics of metabolic networks.

Genome-wide simulation exhibited in this paper is based on the stoichiometry information of genome wide metabolic reactions. Instead of collection of kinetic information of metabolic reactions the principle to solve metabolic fluxes at the steady state is based on that metabolic fluxes should be organized for maximizing the cell growth rate under given environmental conditions. The good agreement of the simulation results with experiments suggests that this principle can represent the direction of the change of metabolic network.

Recently, Almaas et al. showed that the metabolic fluxes of *E.coli* derived by FBA follows the power-law distribution [36]. Even though the FBA does not involve the driving force for representing the dynamics of metabolic networks, the simulated results obtained by genome scale model shows power-law distribution, which are widely found in biological networks. Fursawa and Kaneko independently explained that the origin of the power-law distribution in biological networks is the results of the autonomous organization of the metabolic networks to a critical states maximizing the cell growth based on the simulation based on the cell model with random metabolic reactions [37]. It is interesting that the results of the different types of the models reached the same conclusions concerned with explanation of general characteristic of metabolic network. Further investigations should be performed to unveil characteristic of metabolic network.

4. ACKNOWLEDGMENTS

This work was supported in part by a grant from the Global COE (Centers of Excellence) Program and a grant of special coordination funds for the promotion of science and technology, Yuragi Project, in Osaka University from the Ministry of Education, Culture, Sports, Science and Technology, Japan. This work was also supported by Grant-in-Aid for Young Scientists (B) to CF and TH from the Ministry of Education, Culture, Sports, Science and Technology of Japan.

5. REFERENCES

- [1] Edwards, J.S. and B.O. Palsson, The *Escherichia coli* MG1655 *in silico* metabolic genotype: its definition, characteristics, and capabilities. *Proc Natl Acad Sci U S A*, **97**, 10, (2000) 5528-5533.
- [2] Edwards, J.S., R.U. Ibarra, and B.O. Palsson, *In silico* predictions of *Escherichia coli* metabolic capabilities are consistent with experimental data. *Nat Biotechnol*, **19**, 2 (2001) 125-30.
- [3] Feist, A.M., et al., Modeling methanogenesis with a genome-scale metabolic reconstruction of *Methanosarcina barkeri*. *Mol Syst Biol*, **2** (2006) 2006 0004.
- [4] Feist, A.M., et al., A genome-scale metabolic reconstruction for *Escherichia coli* K-12 MG1655 that accounts for 1260 ORFs and thermodynamic information. *Mol Syst Biol*, **3** (2007) 121.
- [5] Oh, Y.K., et al., Genome-scale reconstruction of metabolic network in *Bacillus subtilis* based on high-throughput phenotyping and gene essentiality data. *J Biol Chem*, **282**, 39, (2007) 28791-28799.
- [6] Thiele, I., et al., Expanded metabolic reconstruction of *Helicobacter pylori* (iT341 GSM/GPR): an *in silico* genome-scale characterization of single- and double-deletion mutants. *J Bacteriol*, **187**, 16 (2005) 5818-5830.
- [7] Oliveira, A.P., J. Nielsen, and J. Forster, Modeling *Lactococcus lactis* using a genome-scale flux model. *BMC Microbiol*, **5** (2005) 39.
- [8] Duarte, N.C., M.J. Herrgard, and B.O. Palsson, Reconstruction and validation of *Saccharomyces cerevisiae* iND750, a fully compartmentalized genome-scale metabolic model. *Genome Res*, **14**, 7 (2004) 1298-1309.
- [9] Sheikh, K., J. Forster, and L.K. Nielsen, Modeling hybridoma cell metabolism using a generic genome-scale metabolic model of *Mus musculus*. *Biotechnol Prog*, **21**, 1, (2005) 112-121.
- [10] Duarte, N.C., et al., Global reconstruction of the human metabolic network based on genomic and bibliomic data. *Proc Natl Acad Sci U S A*, **104**, 6 (2007) 1777-1782.
- [11] Ibarra, R.U., J.S. Edwards, and B.O. Palsson, *Escherichia coli* K-12 undergoes adaptive evolution to achieve *in silico* predicted optimal growth. *Nature*, **420**, 6912(2002) 186-189.
- [12] Fong, S.S. and B.O. Palsson, Metabolic gene-deletion strains of *Escherichia coli* evolve to computationally predicted growth phenotypes. *Nat Genet*, **36**, 10 (2004) 1056-1058.
- [13] Lee, S.J., et al., Metabolic engineering of *Escherichia coli* for enhanced production of succinic acid, based on genome comparison and *in silico* gene knockout simulation. *Appl Environ Microbiol*, **71**, 12 (2005) 7880-7887.
- [14] Alper, H., K. Miyaoku, and G. Stephanopoulos, Construction of lycopene-overproducing *E. coli* strains by combining systematic and combinatorial gene knockout targets. *Nat Biotechnol*, **23**, 5, (2005) 612-616.
- [15] Kinoshita, S., S. Udaka, and M. Shimono, Studies on the amino acid fermentation. *Appl. Microbiol. Jpn.*, **3**, (1957) 193-205.
- [16] Nakayama, K., Kitada, S., and Kinoshita, S., Studies on lysine fermentation. I. The control mechanism on lysine accumulation by homoserine and threonine. *J. Gen. Appl. Microbiol*, **7** (1961) 145-154.
- [17] Leuchtenberger, W., K. Huthmacher, and K. Drauz, Biotechnological production of amino acids and derivatives: current status and prospects. *Appl Microbiol Biotechnol*, **69**, 1, (2005) 1-8.
- [18] Okino, S., M. Inui, and H. Yukawa, Production of organic acids by *Corynebacterium glutamicum* under oxygen deprivation. *Appl Microbiol Biotechnol*, **68**, 4 (2005) 475-80.

- [19] Stephanopoulos, G., *Metabolic fluxes and metabolic engineering*. *Metab Eng*, **1**, 1 (1999) 1-11.
- [20] Shirai, T., et al., Study on roles of anaplerotic pathways in glutamate overproduction of *Corynebacterium glutamicum* by metabolic flux analysis. *Microb Cell Fact*, **6** (2007) 19.
- [21] Karp, P.D., et al., Expansion of the BioCyc collection of pathway/genome databases to 160 genomes. *Nucleic Acids Res*, **33**, 19 (2005) 6083-6089.
- [22] Eggeling, L. and M. Bott, *Handbook of Corynebacterium glutamicum*. (2005) Boca Raton: CRC Press.
- [23] Vallino, J.J. and G. Stephanopoulos, Metabolic flux distributions in *Corynebacterium glutamicum* during growth and lysine overproduction. *Biotechnol Bioeng* **67**, 6, (2000) 872-885 .
- [24] Cocaign-Bousquet, M., A. Guyonvarch, and N.D. Lindley, Growth rate-dependent modulation of carbon flux through central metabolism and the kinetic consequences for glucose-limited chemostat cultures of *Corynebacterium glutamicum*. *Appl Environ Microbiol*, **62**, 2 (1996) 429-436.
- [25] Hoischen, C. and R. Kramer, Membrane alteration is necessary but not sufficient for effective glutamate secretion in *Corynebacterium glutamicum*. *J Bacteriol*, **172**, 6 (1990) 3409-3416.
- [26] Vuorio, R., et al., A new rapidly growing mycobacterial species, *Mycobacterium murale* sp. nov., isolated from the indoor walls of a children's day care centre. *Int J Syst Bacteriol*, **49**, Pt 1 (1999) 25-35.
- [27] Ingraham, J.L., O. Maaloe, and F.C. Neidhardt, *Growth of the bacterial cell*. (1983) Sinauer Associates Inc.
- [28] Ikeda, M. and S. Nakagawa, The *Corynebacterium glutamicum* genome: features and impacts on biotechnological processes. *Appl Microbiol Biotechnol*, **62**, 2-3 (2003) 99-109.
- [29] Kalinowski, J., et al., The complete *Corynebacterium glutamicum* ATCC 13032 genome sequence and its impact on the production of L-aspartate-derived amino acids and vitamins. *J Biotechnol*, **104**, 1-3 (2003) 5-25.
- [30] Crick, D.C., S. Mahapatra, and P.J. Brennan, Biosynthesis of the arabinogalactan-peptidoglycan complex of *Mycobacterium tuberculosis*. *Glycobiology*, **11**, 9 (2001) 107R-118R.
- [31] Kacem, R., et al., Importance of mycoloyltransferases on the physiology of *Corynebacterium glutamicum*. *Microbiology*, **150**, Pt 1 (2004) 73-84.
- [32] Marx, A., et al., Determination of the fluxes in the central metabolism of *Corynebacterium glutamicum* by nuclear magnetic resonance spectroscopy combined with metabolite balancing. *Biotechnol Bioeng*, **49**, 2 (2000) 111-129.
- [33] Shirai, T., et al., Comparative study of flux redistribution of metabolic pathway in glutamate production by two coryneform bacteria. *Metab Eng*, **7**, 2 (2005) 59-69.
- [34] Reed, J.L., et al., An expanded genome-scale model of *Escherichia coli* K-12 (iJR904 GSM/GPR). *Genome Biol*, **4**, 9 (2003) R54.
- [35] Sauer, U., et al., Metabolic flux ratio analysis of genetic and environmental modulations of *Escherichia coli* central carbon metabolism. *J Bacteriol*, **181**, 21 (1999) 6679-6688.
- [36] E. Almaas, B. Kovacs, T. Vicsek, Z.N. Oltvai and A.-L. Barabási, Global organization of metabolic fluxes in the bacterium *Escherichia coli*, *Nature*, **427** (2008), 839-843.
- [37] Furusawa, C. Kaneko, K. Zipf's law in gene expression , *Physical Review Lett*, **90**, 8 (2003) 088102